Possible existence of a bound state in $_\Sigma^7$Li

T. Yamada
Department of Applied Science, Kochi Women's University, Kochi 780, Japan

K. Ikeda
Department of Physics, Niigata University, Niigata 950-21, Japan
and The Institute of Physical and Chemical Research, Wako 351-01, Japan
(Received 4 May 1992)

The possible existence of a bound $_\Sigma^7$Li state is investigated within the frame of the microscopic $\alpha +$ "$2N$" $+\Sigma$ cluster model by employing an effective Σ-N interaction which reproduces the experimental binding energy and width of $_\Sigma^4$He. We found one bound state of $_\Sigma^7$Li with about a 1.2 MeV binding energy and about a 5.4 MeV width, which is composed mainly of $[^6{\rm Li(g.s.)}\otimes\Sigma^0]$ and $[^6{\rm He(g.s.)}\otimes\Sigma^+]$ configurations. It is emphasized that the $(\mathbf{t}_N\cdot\mathbf{t}_\Sigma)(\mathbf{s}_N\cdot\mathbf{s}_\Sigma)$ term of Σ-N interaction plays an important role to produce the bound state. If the bound state is observed in a strangeness exchange reaction such as a $^7{\rm Li}(K^-,\pi^-)_\Sigma^7{\rm Li}$ experiment, we can get direct information on the $(\mathbf{t}_N\cdot\mathbf{t}_\Sigma)$ $(\mathbf{s}_N\cdot\mathbf{s}_\Sigma)$ term of Σ-N interaction.

PACS number(s): 21.80.+a, 14.20.Jn, 21.60.Gx

I. INTRODUCTION

One of the open problems in Σ hypernuclear physics is why the conversion and escaping widths of Σ hypernuclei are so small in spite of the fact that (1) the Σ particle in nuclear matter is immediately converted to a Λ particle because of the strong interaction and (2) the Σ hypernuclear states observed at CERN [1] and BNL [2] are embedded in the continuum region [3–5]. This problem has attracted much theoretical interest [6–11]. However, it still remains unsolved. The presence of the Σ escaping process makes the width problem more complicated. If Σ hypernuclear bound states, in particular, the ground state, are observed, we can know directly the conversion width from the experimental data because of no escaping width. Therefore, it is extremely important to search for bound Σ-hypernuclear states.

Recently, Hayano et al. [12] succeeded in observing the bound Σ-hypernuclear state of $_\Sigma^4$He for the first time through the (stopped K^-, π^-) experiment on a target of ^{4}He at KEK. The experimental binding energy ($B_{\Sigma^+}=3.2$ MeV) and width ($\Gamma=4.6\pm0.5^{+1.6}_{-1.3}$ MeV) of $_\Sigma^4$He have provided us with important information on the sigma (Σ)-nucleon (N) interaction. The four-body $NNN\Sigma$ model [13] and the $[^3{\rm H}+\Sigma^+]+[^3{\rm He}+\Sigma^0]$ model [14,15] were applied to the study of the structure of $_\Sigma^4$He on the basis of the Nijmegen model D potential [16]. They showed that the bound $_\Sigma^4$He state is an almost pure isospin $I\approx\frac12$ state reflecting the strong repulsive so-called Lane potential between the Σ particle and nuclear core. We pointed out [15] that (1) the Lane potential comes from the constructive contribution from the $(\mathbf{t}_N\cdot\mathbf{t}_\Sigma)$ and $(\mathbf{t}_N\cdot\mathbf{t}_\Sigma)(\mathbf{s}_N\cdot\mathbf{s}_\Sigma)$ terms of Σ-N interaction, and that (2) the contribution from the $(\mathbf{t}_N\cdot\mathbf{t}_\Sigma)(\mathbf{s}_N\cdot\mathbf{s}_\Sigma)$ term to the Lane potential is about twice as large as that from the $(\mathbf{t}_N\cdot\mathbf{t}_\Sigma)$ term.

It is an interesting problem to see whether bound states and /or quasibound states could exist in other light Σ hypernuclei by using the effective Σ-N interaction which reproduces the experimental data of $_\Sigma^4$He [15]. In this paper, we investigate the possible existence of bound states in the $_\Sigma^7$Li hypernucleus and clarify their binding mechanism. The low-lying states of the $A=6$ body nuclear core (^{6}He-^{6}Li-^{6}Be) of $_\Sigma^7$Li have two spin-isospin groups, $(s,t)=(1,0)$ and $(0,1)$, whose states are known approximately to form a supermultiplet. The different charge states which are composed of Σ particles (Σ^+, Σ^0, Σ^-) and the corresponding supermultiplet of the $A=6$ body nuclear system are coupled by the isospin-dependent $(\mathbf{t}_N\cdot\mathbf{t}_\Sigma)$ and isospin-spin-dependent $(\mathbf{t}_N\cdot\mathbf{t}_\Sigma)(\mathbf{s}_N\cdot\mathbf{s}_\Sigma)$ terms of Σ-N interaction. It is interesting to see what kinds of coupling mechanisms are actually realized in the $_\Sigma^7$Li hypernucleus. Since the low-lying structure of the $A=6$ body nuclear system is known to be described nicely by the microscopic $\alpha +$ "$2N$" cluster model, the structure of $_\Sigma^7$Li is studied with use of the microscopic $\alpha +$ "$2N$" $+\Sigma$ cluster model. As the effective Σ-N interaction, we employ the YNG-D interaction [17] constructed on the basis of the G-matrix calculation for the Nijmegen model D potential [16]. This effective interaction is adjusted to reproduce the experimental binding energy and width of $_\Sigma^4$He by performing the structure analysis using the $[^3{\rm H}+\Sigma^+]+[^3{\rm He}+\Sigma^0]$ model [15].

In Sec. II, the microscopic $\alpha +$ "$2N$" $+\Sigma$ cluster model is formulated. The results and discussion are given in Sec. III. Finally, we present conclusions in Sec. IV.

II. FORMULATION

A. Microscopic $\alpha +$ "$2N$" $+\Sigma$ cluster model for $_\Sigma^7$Li

The low-lying states of the $A=6$ body nuclear system (^{6}He-^{6}Li-^{6}Be) could be classified into two groups,

$(s,t)=(1,0)$ and $(0,1)$, where s and t denote the total spin and isospin of the $A=6$ body nuclear system, respectively. Since the Σ particle has three charge states $(t_\Sigma=1)$, we consider the following four basic charge states with the same charge for a ${}^7_\Sigma\text{Li}$ hypernuclear state: (1) $[{}^6\text{He}(s=0, t=1)\otimes\Sigma^+]$, (2) $[{}^6\text{Li}(s=0, t=1)\otimes\Sigma^0]$, (3)

$[{}^6\text{Be}(s=0, t=1)\otimes\Sigma^-]$, and (4) $[{}^6\text{Li}(s=1, t=0)\otimes\Sigma^0]$.

Within the frame of the microscopic $\alpha+\text{"}2N\text{"}+\Sigma$ cluster model, the total wave function of a ${}^7_\Sigma\text{Li}$ state with the total angular momentum J and the total isospin z-component $T_z=0$ is expressed as

$$\Psi_J({}^7_\Sigma\text{Li})= \sum_{c,d,D} w_c(d,D)\{|\Phi_{lsjtm}(d)\rangle|\varphi_\lambda(R;D)[Y_\lambda(\hat{R})s_\Sigma]_{j_\Sigma}t_\Sigma-m\rangle\}_J ,\qquad(2.1)$$

$$c=((l,s)_j,(\lambda,s_\Sigma=\tfrac{1}{2})_{j_\Sigma};J(t,t_\Sigma=1),m) ,\qquad(2.2)$$

where $w_c(d,D)$ is an expansion coefficient and c denotes a channel of the basic charge state and the angular momentum coupling. The $(\alpha+\text{"}2N\text{"})-\Sigma$ relative wave function is expanded into the Gaussian wave packet

$$\varphi_\lambda(R;D)=4\pi(\pi b_R^2)^{-3/4}\exp[-(R^2+D^2)/2b_R^2]$$

$$\times \mathcal{J}_\lambda(RD/b_R^2) ,\qquad(2.3)$$

where λ is the relative orbital angular momentum referring to the relative coordinate R between the Σ particle and the center-of-mass of the $\alpha+\text{"}2N\text{"}$ part, and s_Σ and t_Σ $(-m)$ represent the spin and isospin (isospin z component) of the Σ particle. The generator coordinate D in Eq. (2.3) denotes the distance between the $\alpha+\text{"}2N\text{"}$ and Σ parts, and $\mathcal{J}_\lambda(z)$ is the spherical Bessel function with an imaginary argument. The size parameter b_R is chosen to give the same harmonic oscillator frequency Ω as for nucleons. For the $\alpha+\text{"}2N\text{"}$ part, we employ the generator coordinate basic wave function $\Phi_{lsjtm}(d)$ which is given by

$$\Phi_{lsjtm}(d)=\sqrt{4!2!/6!}\,\mathcal{A}'\{\phi_\alpha\phi_{2N}(s;tm)\varphi_l(r;d)Y_l(\hat{r})\}_j ,$$

$$(2.4)$$

where j and l denote, respectively, the total angular momentum and the relative orbital angular momentum referring to the relative coordinate r between the α and "$2N$" clusters. ϕ_α and $\phi_{2N}(s;tm)$ represent the intrinsic wave functions of α and "$2N$" clusters with the harmonic oscillator $(0s)^4$ and $(0s)^2$ configurations, respectively. The operator $\mathcal{A}'$ in Eq. (2.4) antisymmetrizes the nucleons belonging to different clusters. The generator coordinate d in the Gaussian wave packet $\varphi_l(r;d)$ in Eq. (2.4) denotes the $\alpha-\text{"}2N\text{"}$ distance. Here, we note that the wave function $\varphi_l(r;d)$ has only the harmonic oscilla-

tor basis with principal quantum number $N\geq2$ due to the antisymmetrization.

The total Hamiltonian of the $\alpha+\text{"}2N\text{"}+\Sigma$ system is given by

$$H=H_{\alpha-2N}+T_R+V_{\Sigma N}+V_{\text{Coul}}+(\Delta M)_{c,c'} ,\qquad(2.5)$$

$$V_{\Sigma N}=\sum_{n=1}^{6} v_{\Sigma N}(\Sigma,n),\quad V_{\text{Coul}}=\sum_{n=1}^{6} v_{\text{Coul}}(\Sigma,n) ,\qquad(2.6)$$

where $H_{\alpha-2N}$, T_R, and $V_{\Sigma N}$ (V_{Coul}) represent the Hamiltonian of the $\alpha+\text{"}2N\text{"}$ part, the relative kinetic energy between the Σ particle and the center of mass of the $\alpha+\text{"}2N\text{"}$ part of the Σ-N strong (Coulomb) interactions, respectively. The mass difference matrix $(\Delta M)_{c,c'}$ in Eq. (2.5) is diagonal and is given as follows:

$\Delta M=M(\Sigma^+)-M(\Sigma^0)+M({}^6\text{He})-M({}^6\text{Li})=0.96$ MeV

for the ${}^6\text{He}(s=0, t=1)+\Sigma^+$ channel,

$\Delta M=M({}^6\text{Li}(0^+))-M({}^6\text{Li})=3.56$ MeV

for the ${}^6\text{Li}(s=0, t=1)+\Sigma^0$ channel,

$\Delta M=M(\Sigma^-)-M(\Sigma^0)+M({}^6\text{Be})-M({}^6\text{Li})=8.66$ MeV

for the ${}^6\text{Be}(s=0, t=1)+\Sigma^-$ channel, and

$\Delta M=0.0$ MeV

for the ${}^6\text{Li}(s=1, t=0)+\Sigma^0$ channel. Here $M(\Sigma^{\pm,0})$ denote the masses of Σ particles, and $M({}^6\text{He})$, $M({}^6\text{Li})$, $M({}^6\text{Be})$, and $M({}^6\text{Li}(0^+))$ express the masses of the ground states of ${}^6\text{He}$, ${}^6\text{Li}$, and ${}^6\text{Be}$ and of the ${}^6\text{Li}(0^+;3.56$ MeV) state, respectively.

The equation of motion for the $\alpha+\text{"}2N\text{"}+\Sigma$ system is derived from the variational principle and given as the coupled-channel secular equation for the expansion coefficient $w_c(d,D)$:

$$\sum_{c_2d_2D_2} \{\delta_{c_1c_2}[N_{l_1s_1j_1t_1}^{\alpha-2N}(d_1,d_2)T_{\lambda_1}^{\Sigma}(D_1,D_2)+H_{l_1s_1j_1t_1}^{\alpha-2N}(d_1,d_2)N_{\lambda_1}^{\Sigma}(D_1,D_2)+(E_J-(\Delta M)_{c_1c_2})N_{l_1s_1j_1t_1}^{\alpha-2N}(d_1,d_2)N_{\lambda_1}^{\Sigma}(D_1,D_2)]$$

$$+U_J^{\Sigma N}(c_1d_1D_1;c_2d_2D_2)\}w_{c_2}(d_2,D_2)=0 ,\qquad(2.7)$$

$$H_{lsjt}^{\alpha-2N}(d_1,d_2)=\langle\Phi_{lsjt}(d_1)|H_{\alpha-2N}|\Phi_{lsjt}(d_2)\rangle ,\qquad(2.8)$$

$$N_{lsjt}^{\alpha-2N}(d_1,d_2)=\langle\Phi_{lsjt}(d_1)|\Phi_{lsjt}(d_2)\rangle ,\qquad(2.9)$$

$$T_\lambda^{\Sigma}(D_1,D_2)=\langle\varphi_\lambda(R;D_1)|T_R|\varphi_\lambda(R;D_2)\rangle ,\qquad(2.10)$$

$$N_\lambda^{\Sigma}(D_1,D_2)=\langle\varphi_\lambda(R;D_1)|\varphi_\lambda(R;D_2)\rangle ,\qquad(2.11)$$

$$U_J^{\Sigma N}(c_1 d_1 D_1; c_2 d_2 D_2)$$

$$= \langle [\Phi_{l_1 s_1 j_1 t_1 m_1}(d_1)\varphi_{\lambda_1}(R;D_1)][Y_{\lambda_1}(\hat{R})s_\Sigma]_{j_{\Sigma_1}} t_\Sigma - m_1]_J | V_{\Sigma N} | [\Phi_{l_2 s_2 j_2 t_2 m_2}(d_2)\varphi_{\lambda_2}(R;D_2)][Y_{\lambda_2}(\hat{R})s_\Sigma]_{j_{\Sigma_2}} t_\Sigma - m_2]_J \rangle \ .$$

$$(2.12)$$

The Σ-nucleus potential given in Eq. (2.12) is complex quantity since the Σ-N interaction has the imaginary part which simulates the $\Sigma N \to \Lambda N$ conversion process as shown in Sec. II B. It is noted that the presence of the isospin-dependent terms in Σ-N interaction causes the coupling among the different basic charge states.

The basic wave function $\Phi_{lsjt}(d)$ given in Eq. (2.4) can be expanded in terms of the normalized-antisymmetrized harmonic oscillator basis $\Phi_{lsjt}^{\text{h.o.}}(n)$;

$$\Phi_{lsjt}(d) = \sum_n \sqrt{\mu_N} a_{nl}(d,b_r) \Phi_{lsjt}^{\text{h.o.}}(n) \ ,$$

$$(2.13)$$

$$a_{nl}(d,b_r) = \frac{\sqrt{2}\pi^{3/4}(-1)^n}{\{\Gamma(n+l+3/2)\Gamma(n+1)\}^{1/2}}(\sqrt{\nu/2}\,d)^{2n+l}\exp\left[-\frac{\nu}{2}d^2\right] \ ,$$

$$(2.14)$$

$$\Phi_{lsjt}^{\text{h.o.}}(n) = \frac{1}{\sqrt{\mu_N}}\sqrt{4!2!/6!}\,\mathcal{A}'\{\phi_\alpha \phi_{2N}(st)u_{nl}(r)Y_l(\hat{r})\}_j \ ,$$

$$(2.15)$$

where $u_{nl}(r)$ is the harmonic oscillator wave function with size b_r and quanta $N = 2n + l$, and μ_N denotes the normalization factor. Then, the Hamiltonian and norm kernels of the $\alpha + $ "$2N$" nuclear system defined in Eqs. (2.8) and (2.9) are, respectively, expressed as

$$H_{lsjt}^{\alpha - 2N}(d_1, d_2) = \sum_{n_1, n_2} \sqrt{\mu_{N_1}\mu_{N_2}} a_{n_1 l}(d_1, b_r) a_{n_2 l}(d_2, b_r) \langle \Phi_{lsjt}^{\text{h.o.}}(n_1) | H_{\alpha - 2N} | \Phi_{lsjt}^{\text{h.o.}}(n_2) \rangle \ ,$$

$$(2.16)$$

$$N_{lsjt}^{\alpha - 2N}(d_1, d_2) = \sum_n \mu_N a_{nl}(d_1, b_r) a_{nl}(d_2, b_r) \ .$$

$$(2.17)$$

The Hamiltonian kernel in Eq. (2.16) is calculated with use of the OCM (orthogonality condition model) [18,19] approximation:

$$\langle \Phi_{lsjt}^{\text{h.o.}}(n_1) | H_{\alpha - 2N} | \Phi_{lsjt}^{\text{h.o.}}(n_2) \rangle \to \langle u_{n_1} lsjt | H_{\alpha - 2N}^{\text{OCM}} | u_{n_2} lsjt \rangle \ .$$

$$(2.18)$$

Here, the OCM effective Hamiltonian $H_{\alpha - 2N}^{\text{OCM}}$ consists of the relative kinetic energy and the central, spin-orbit, and Coulomb potentials between the α and "$2N$" clusters,

$$H_{\alpha - 2N}^{\text{OCM}} = T_r + V_C(r) + V_{LS}(r) + V_{\text{Coul}}(r) \ .$$

$$(2.19)$$

For $V_C(r)$ and $V_{LS}(r)$, range-1 Gaussian effective potentials are used,

$$V_C(r) = V_C^0 \exp[-(r/\beta_C)^2] \ ,$$

$$(2.20)$$

$$V_{LS}(r) = V_{LS}^0 \exp[-(r/\beta_{LS})^2](l \cdot s) \ ,$$

$$(2.21)$$

and, for $V_{\text{Coul}}(r)$, the direct Coulomb potential is employed as

$$V_{\text{Coul}}(r) = \frac{Z_1 Z_2 e^2}{r} \text{erf}(r/b_c), \quad b_c = \sqrt{\tfrac{5}{4}} b_N \ ,$$

$$(2.22)$$

where $Z_1 = 2$ for α and Z_2 is the number of protons in the "$2N$" cluster and b_N denotes the nucleon size parameter.

For later discussions, it is useful to define the Σ-particle reduced-width amplitude for the $\Psi_J(^{7}_{\Sigma}\text{Li})$ state as

$$\mathcal{Y}_{lsjtm,\lambda j_\Sigma, J}^{\Sigma -(A=6)}(R) = R \langle [\Phi_{lsjtm}(A=6)[Y_\lambda(\hat{R})s_\Sigma]_{j_\Sigma} t_\Sigma - m]_J | \Psi_J(^{7}_{\Sigma}\text{Li}) \rangle \ ,$$

$$(2.23)$$

where $\Phi_{lsjtm}(A = 6)$ denotes the $A = 6$ body nuclear wave function obtained by the $\alpha + $ "$2N$" OCM calculation with the Hamiltonian given in Eq. (2.19).

B. Σ-N interaction

As the effective Σ-N interaction, we use the YNG-D interaction [17] derived from the G-matrix calculation based on the Nijmegen model D potential [16]. The

YNG-D Σ-N interaction with the three-range Gaussian form is a complex quantity and the imaginary part simulates the conversion process $\Sigma N \to \Lambda N$:

$$v_{\Sigma N}(r) = v_{\Sigma N}^0(r;k_F) + v_{\Sigma N}^\tau(r;k_F)(t_N \cdot t_\Sigma)$$

$$+ v_{\Sigma N}^\sigma(r;k_F)(s_N \cdot s_\Sigma) + v_{\Sigma N}^{\tau\sigma}(r;k_F)(t_N \cdot t_\Sigma)(s_N \cdot s_\Sigma) \ .$$

$$(2.24)$$

TABLE I. Parameters of the central and spin-orbit potentials between the alpha and "$2N$" clusters.

(s,t)	V_C^0 (MeV)	β_C (fm)	V_{LS}^0 (MeV)	β_{LS} (fm)
(1,0)	−74.2	2.236	−7.0	1.826
(0,1)	−66.7	2.236		

In the present study, we assume that the nuclear Fermi momentum k_F is an adjustable parameter since it may not make sense to use the local density approximation seriously in light systems such as a $_\Lambda^7$Li hypernucleus. The value of k_F is determined so as to reproduce the experimental binding energy and width of $_\Lambda^4$He [12] by performing the structure analysis within the frame of the $[^3\mathrm{H}+\Sigma^+]+[^3\mathrm{He}+\Sigma^0]$ model [15]. According to Ref. [15], we set $k_F = 0.86$ fm^{-1} which gives the calculated binding energy ($B_\Sigma^{\mathrm{cal}} = 3.2$ MeV vs $B_\Sigma^{\mathrm{exp}} = 3.2$ MeV) and width ($\Gamma^{\mathrm{cal}} = 7.8$ MeV vs $\Gamma^{\mathrm{exp}} = 4.6 \pm 0.5^{+1.6}_{-1/3}$ MeV) of $_\Lambda^4$He.

For later discussions, it is useful to give the sum of Σ-N interaction defined in Eq. (2.6) as

$$V_{\Sigma N} = 1 + (\mathbf{T}_N \cdot \mathbf{t}_\Sigma) + (\mathbf{S}_N \cdot \mathbf{s}_\Sigma) + (\mathbf{Y}_N \cdot \mathbf{y}_\Sigma) , \qquad (2.25)$$

$$1 = \sum_{n=1}^6 v_{\Sigma N}^0(\Sigma, n), \quad \mathbf{T}_N = \sum_{n=1}^6 v_{\Sigma N}^\tau(\Sigma, n)\mathbf{t}_n ,$$

$$\mathbf{S}_N = \sum_{n=1}^6 v_{\Sigma N}^\sigma(\Sigma, n)\mathbf{s}_n ,$$

$$\mathbf{Y}_N = \sum_{n=1}^6 v_{\Sigma N}^{\tau\sigma}(\Sigma, n)\mathbf{t}_n\mathbf{s}_n , \qquad (2.26)$$

where $\mathbf{y}_\Sigma$ is defined as $\mathbf{t}_\Sigma \mathbf{s}_\Sigma$.

C. Model space

For the $\alpha +$ "$2N$" part, we use the following model space: (1) the $\alpha -$ "$2N$" orbital angular momentum $l = 0,2$, (2) the GCM mesh points $d = 1.2$, 2.4, 3.6, 4.8, 6.0 fm, and (3) the number of node for the harmonic oscillator basis when making the OCM approximation $n = 0, 1, \ldots, 9$. This model space is enough to describe the low-lying structure of the $A = 6$ body nuclear system. The nucleon size parameter b_N is chosen to be 1.358 fm. This value has been employed in the systematic structure

study of the p-shell Λ hypernuclei within the frame of the microscopic cluster model [20]. For the potential parameters defined in Eqs. (2.20) and (2.21), we use the parameter values so as to reproduce the experimental energy spectra of the $A = 6$ body nuclear system [21]. (See Table I.)

Figure 1 shows the calculated energy spectra of the $A = 6$ body nuclear system in comparison with the experimental $A = 6$ isobar diagram [22]: $j^\pi = 1^+$ ($l = 0$, $s = 1$, $t = 0$), $j^\pi = 3^+ - 2^+ - 1^+$ ($l = 2$, $s = 1$, $t = 0$), $j^\pi = 0^+$ ($l = 0$, $s = 0$, $t = 1$), and $j^\pi = 2^+$ ($l = 2$, $s = 0$, $t = 1$) for ^{6}Li; $j^\pi = 0^+$ ($l = 0$, $s = 0$, $t = 1$) and $j^\pi = 2^+$ ($l = 2$, $s = 0$, $t = 1$) for ^{6}He and ^{6}Be. The calculated results are in good agreement with the experimental data for the $(s,t) = (1,0)$ and $(s,t) = (0,1)$ states.

The following model space is used to obtain the eigenenergy and eigen-wave-function of $_\Lambda^7$Li.

(1) The charge bases:

$[^6\mathrm{He} \otimes \Sigma^+]$ with $(l,s)_j t = (0,0)_0 1$ and $(2,0)_2 1$,

$[^6\mathrm{Li} \otimes \Sigma^0]$ with $(l,s)_j t = (0,0)_0 1$ and $(2,0)_2 1$,

$[^6\mathrm{Be} \otimes \Sigma^-]$ with $(l,s)_j t = (0,0)_0 1$ and $(2,0)_2 1$,

$[^6\mathrm{Li} \otimes \Sigma^0]$ with $(l,s)_j t = (0,1)_1 0$ and $(2,1)_{1,2,3} 0$.

(2) The GCM mesh points for the $\alpha +$ "$2N$" part:

$d = 1.2$, 2.4, 3.6, 4.8, 6.0 fm .

(3) The GCM mesh points for the $(\alpha +$ "$2N$"$) - \Sigma$ part:

$D = 0.5$, 1.3, 2.1, 2.9, 3.7, 4.5, 5.2, 6.0, 6.8, 7.6 .

(4) The relative orbital angular momentum referring to the $(\alpha +$ "$2N$"$) - \Sigma$ part: $\lambda = 0, 2$.

It should be noted that the model space for the $\alpha +$ "$2N$" part is the same as that employed in the case of the $A = 6$ body nuclear system as mentioned above. The present model space is considered to be enough to describe low-lying states of $_\Lambda^7$Li.

III. RESULTS AND DISCUSSION

Adding Σ particles (Σ^+, Σ^0, and Σ^-) to the isobar-diagram of the $A = 6$ body nuclear system (Fig. 2(a) [22]) and taking into account the mass differences among
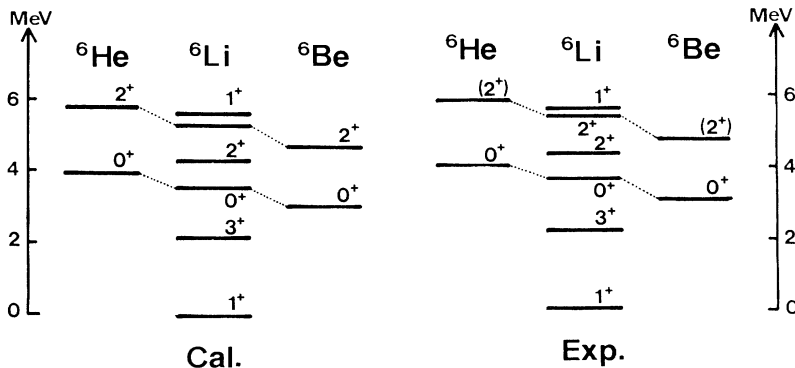

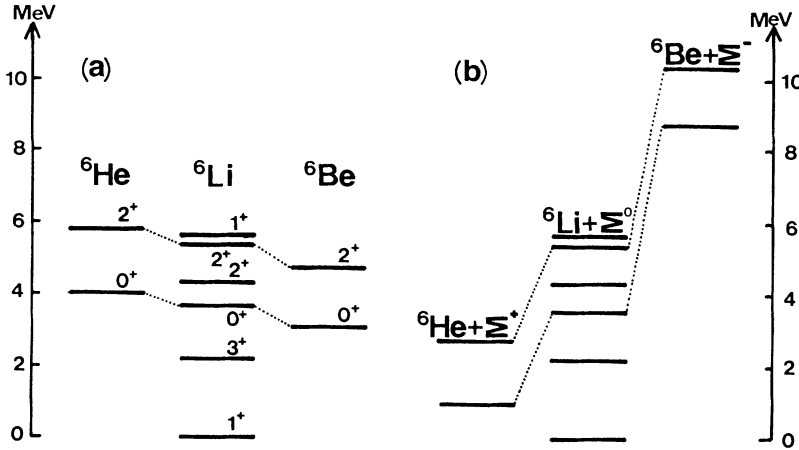FIG. 1. Calculated energy spectra of the $A = 6$ body nuclear system together with the experimental data [22].

FIG. 2. (a) Isobar-diagram of the $A=6$ body nuclear system [22], and (b) various Σ particle decay thresholds for $^7_\Sigma$Li.

Σ particles, the mass difference between proton and neutron, and the Coulomb energy differences among nuclear cores, we get the Σ-particle decay thresholds of the $^7_\Sigma$Li hypernucleus as shown in Fig. 2(b). It should be noted that the drastic change from Fig. 2(a) to Fig. 2(b) is mainly due to the mass differences among Σ^+ (1189.4 MeV), Σ^0 (1192.5 MeV) and Σ^- (1197.3 MeV). The threshold energy difference between the ^{6}He(0_1^+)+Σ^+ and ^{6}Li(1_1^+)+Σ^0 channels is only about 0.96 MeV, while the energy difference between the ^{6}He(0_1^+) and ^{6}Li(1_1^+) states is about 4.1 MeV.

If eigenstates of $^7_\Sigma$Li appear below the ^{6}Li(1_1^+)+Σ^0 threshold, they become bound states. After diagonalization of the many coupled-channel equations given in Eq. (2.7), we found only one bound state with $J^\pi=\frac{1}{2}^+$ which corresponds to the ground state of $^7_\Sigma$Li. Other higher J^π states have not been obtained as bound states in the present calculation. The calculated binding energy of the bound $J^\pi=\frac{1}{2}^+$ state is $B_{\Sigma^0}=1.2$ MeV, which is measured from the ^{6}Li(1_1^+)+Σ^0 threshold, and the calculated conversion width is $\Gamma\approx5.4$ MeV. Note that both the calculated binding energy and conversion width of $^7_\Sigma$Li are smaller than those of $^4_\Sigma$He ($B^{calc}_{\Sigma^+}=3.2$ MeV and $\Gamma^{calc}=7.8$ MeV). The obtained wave function is expressed as

$$\Psi(^7_\Sigma\text{Li})=\sqrt{0.66}[^6\text{Li}(1_1^+)\otimes\Sigma^0(s_{1/2})]$$

$$+\sqrt{0.27}[^6\text{He}(0_1^+)\otimes\Sigma^+(s_{1/2})]+\cdots \quad (3.1a)$$

$$=\sqrt{0.11}|I=0\rangle+\sqrt{0.83}|I=1\rangle+\sqrt{0.06}|I=2\rangle . \quad (3.1b)$$

The bound state shows the mixed charge state with about 83% of the total isospin $I=1$ component ($\mathbf{I}=\mathbf{t}+\mathbf{t}_\Sigma$). This is in contrast with the fact that the bound $^4_\Sigma$He state is an almost pure isospin-$\frac{1}{2}$ state (about 99%).

The reason why such a bound $^7_\Sigma$Li state appears is given as follows: In the relevant state, it is instructive to illustrate the four charge states, $[^6\text{He}(0_1^+)\otimes\Sigma^+]$, $[^6\text{Li}(1_1^+)\otimes\Sigma^0]$, $[^6\text{Li}(0_1^+)\otimes\Sigma^0]$, and $[^6\text{Be}(0_1^+)\otimes\Sigma^-]$, since they play an important role in producing the bound state as shown below. Figure 3(a) demonstrates the aspect of

the coupling among the four configurations which are caused by the isospin-dependent operator $(\mathbf{T}_N\cdot\mathbf{t}_\Sigma)$ and spin-isospin-dependent operator $(\mathbf{Y}_N\cdot\mathbf{y}_\Sigma)$ of the Σ-N interactions defined in Eq. (2.26). Note that the Wigner and spin-spin terms of Σ-N interactions contribute only to the Σ-nucleus folding potential for each configuration. The operator $(\mathbf{Y}_N\cdot\mathbf{y}_\Sigma)$ makes the $[^6\text{Li}(1_1^+)\otimes\Sigma^0]$ configuration ($s=1$, $t=0$) couple with the $s=0$, $t=1$ configurations $[^6\text{He}(0_1^+)\otimes\Sigma^+]$ and $[^6\text{Be}(0_1^+)\otimes\Sigma^-]$, since the $(\mathbf{Y}_N\cdot\mathbf{y}_\Sigma)$ has the role of flipping simultaneously the nuclear-core isospin and spin by 1. On the other hand, the operator $(\mathbf{T}_N\cdot\mathbf{t}_\Sigma)$ constructs the Lane potential which couples the $[^6\text{He}(0_1^+)\otimes\Sigma^+]$, $[^6\text{Li}(0_1^+)\otimes\Sigma^0]$, and $[^6\text{Be}(0_1^+)\otimes\Sigma^-]$ configurations with the nuclear-core isospin $t=1$, since the $(\mathbf{T}_N\cdot\mathbf{t}_\Sigma)$ has the role of flipping only the nuclear-core isospin by 1 with no change of the nuclear-core spin. It should be noted that there is no coupling between the $[^6\text{Li}(1_1^+)\otimes\Sigma^+]$ and $[^6\text{Li}(0_1^+)\otimes\Sigma^0]$ configurations because of the characteristic of the $(\mathbf{Y}_N\cdot\mathbf{y}_\Sigma)$ and $(\mathbf{T}_N\cdot\mathbf{t}_\Sigma)$ operators. If the coupling strength is enough larger than the energy differences among the four channels, we expect to get supermultiplet states (spin-isospin good quantum number states) of $^7_\Sigma$Li which consist of the four charge states.

Figure 4 shows the Σ-nucleus folding and coupling po-
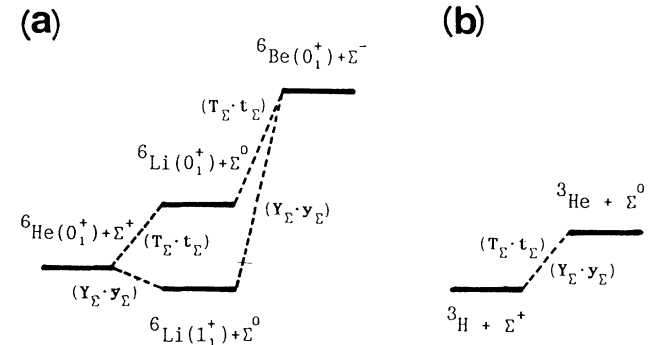

FIG. 3. (a) Couplings among $[^6\text{He}(0_1^+)\otimes\Sigma^+]$, $[^6\text{Li}(1_1^+)\otimes\Sigma^0]$, $[^6\text{Li}(0_1^+)\otimes\Sigma^0]$, and $[^6\text{Be}(0_1^+)\otimes\Sigma^-]$ channels in $^7_\Sigma$Li. (b) Coupling between $[^3\text{H}\otimes\Sigma^+]$ and $[^3\text{He}\otimes\Sigma^0]$ channels in $^4_\Sigma$He.
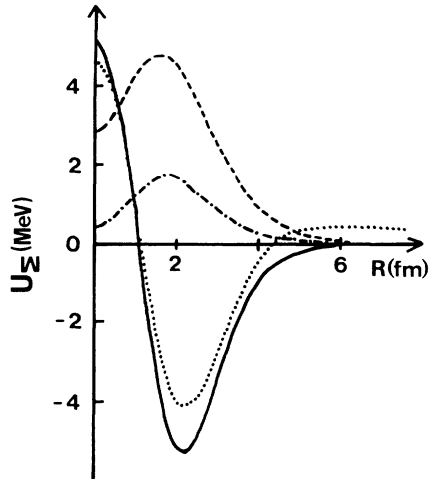
FIG. 4. The solid and dotted lines show the Σ-nucleus folding potentials (including Coulomb potential) for $^6\mathrm{Li}(1_1^+)+\Sigma^0$ and $^6\mathrm{He}(0_1^+)+\Sigma^+$ channels, respectively. The dashed [dash-dotted] line represents the coupling potential between $^6\mathrm{Li}(1_1^+)+\Sigma^0$ and $^6\mathrm{He}(0_1^+)+\Sigma^+$ [$^6\mathrm{He}(0_1^+)+\Sigma^+$ and $^6\mathrm{Li}(0_1^+)+\Sigma^0$] channels.

tentials. The folding potentials for the $^6\mathrm{He}(0_1^+)+\Sigma^+$ and $^6\mathrm{Li}(1_1^+)+\Sigma^0$ channels have a repulsive part in the inner region ($R<1.0$ fm) and a shallow attractive part in the outer region ($R>1.0$ fm). The situation is almost the same in the case of the $^6\mathrm{Li}(0_1^+)+\Sigma^0$ and $^6\mathrm{Be}(0_1^+)+\Sigma^-$ channels. Therefore, each eigenstate with no channel coupling appears around each threshold. On the other hand, as shown in Fig. 4, the coupling potential between the $^6\mathrm{Li}(1_1^+)+\Sigma^0$ and $^6\mathrm{He}(0_1^+)+\Sigma^+$ channels is very large. Its value amounts to about 4 MeV at $R\approx2.0$ fm. The 4-MeV coupling strength is much larger than the energy difference (~ 1 MeV) between each eigenstate. Therefore, the two channels are coupled strongly to produce the bound state. The $^6\mathrm{Be}(0_1^+)+\Sigma^-$ and $^6\mathrm{Li}(1_1^+)+\Sigma^0$ channels are hardly coupled strongly because of the large energy difference between them (~ 9 MeV). In Fig. 4, the coupling potential between the $^6\mathrm{He}(0_1^+)+\Sigma^+$ and $^6\mathrm{Li}(0_1^+)+\Sigma^0$ channels which corresponds to the Lane potential is also shown. Its strength is relatively small in comparison with the energy difference between the two channels. The situation is almost the same as that in the case of the $^6\mathrm{Li}(0_1^+)+\Sigma^0$ and $^6\mathrm{Be}(0_1^+)+\Sigma^-$ channels. Therefore, the $^6\mathrm{He}(0_1^+)+\Sigma^+$, $^6\mathrm{Li}(0_1^+)+\Sigma^0$ and $^6\mathrm{Be}(0_1^+)+\Sigma^-$ channels with the nuclear-core isospin $t=1$ are not strongly coupled with each other. After all, the two channels $^6\mathrm{He}(0_1^+)+\Sigma^+$ and $^6\mathrm{Li}(1_1^+)+\Sigma^0$ are coupled strongly to produce one bound state with $B_{\Sigma^0}=1.2$ MeV which does not correspond to a pure Σ-hypernuclear supermultiplet state. This is a different characteristic from the case of the $^4_\Sigma\mathrm{He}$ bound state with almost pure isospin $\frac{1}{2}$ ($\sim 99\%$) which is produced by the strong coupling between the $^3\mathrm{H}+\Sigma^+$ and $^3\mathrm{He}+\Sigma^0$ channels [13–15]. As emphasized in Ref. [15], the strong coupling comes from the cooperative role of the isospin-dependent operator ($\mathbf{T}_N\cdot\mathbf{t}_\Sigma$) and spin-isospin dependent operator ($\mathbf{Y}_N\cdot\mathbf{y}_\Sigma$) of the Σ-N interac-

tions as shown in Fig. 3(b). Such a situation does not hold in the $^7_\Sigma\mathrm{Li}$ case. It holds only in the special case that the spin and isospin of the nuclear core are $\frac{1}{2}$ and $\frac{1}{2}$ [15].

The calculated conversion width (~ 5.4 MeV) of the $^7_\Sigma\mathrm{Li}$ bound state is much smaller than the conversion width (20–30 MeV) in free space [3] and is smaller than the calculated width of $^4_\Sigma\mathrm{He}$ (~ 7.8 MeV). Yamamoto and Bando [17] pointed out that the conversion width in nuclear matter becomes as small as about 10 MeV due to the effect of the Pauli principle. The reason why the conversion width of $^7_\Sigma\mathrm{Li}$ and $^4_\Sigma\mathrm{He}$ is smaller than that in nuclear matter is attributed to the fact that the $^7_\Sigma\mathrm{Li}$ and $^4_\Sigma\mathrm{He}$ hypernuclei are finite nuclear systems. As is well known, the width in the first-order perturbation theory is given as the integration of the overlap between the Σ-nucleus imaginary potential and the squared Σ-nucleus relative wave function. When the binding energy of Σ particle is smaller (larger), the Σ-nucleus relative wave function has a longer (shorter) tail. Therefore, the smaller (larger) binding energy of the Σ particle gives the smaller (larger) conversion width. This is a general characteristic in Σ hypernuclei. In Fig. 5, we show the squared reduced width amplitudes for the $^6\mathrm{Li}(1_1^+)+\Sigma^0(s_{1/2})$ and $^6\mathrm{He}(0_1^+)+\Sigma^+(s_{1/2})$ channels, and the respective Σ-nucleus imaginary potentials. Both the reduced width amplitudes have long tails. This is due to the fact that the binding energy is as small as about 1.2 MeV and the Σ-nucleus real potentials have the repulsive part in the inner region ($R<1.0$ fm) and the long attractive part in the outer region ($R>1.0$ fm) (see Fig. 4). As a result, the conversion width of $^7_\Sigma\mathrm{Li}$ becomes as small as about 5.4 MeV. On the other hand, the calculated binding energy of $^7_\Sigma\mathrm{Li}$ ($B_{\Sigma^0}=1.2$ MeV) is smaller than that of $^4_\Sigma\mathrm{He}$ ($B_{\Sigma^+}=3.2$ MeV). This means that the Σ-nucleus relative wave function of the $^7_\Sigma\mathrm{Li}$ bound state has a longer tail than that for $^4_\Sigma\mathrm{He}$. Therefore, the calculated width of $^7_\Sigma\mathrm{Li}$ is smaller than that of $^4_\Sigma\mathrm{He}$.

In order to see the relation between the binding energies of $^7_\Sigma\mathrm{Li}$ and $^4_\Sigma\mathrm{He}$, we show in Fig. 6 the dependence of the nuclear Fermi momentum k_F of the YNG-D Σ-N interaction [see Eq. (2.24)] on the binding energies of $^7_\Sigma\mathrm{Li}$ and $^4_\Sigma\mathrm{He}$. When the value of k_F is taken from 0.8 to 1.0
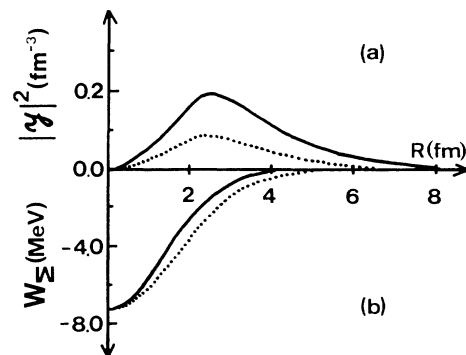

FIG. 5. (a) Squared reduced width amplitudes for $^6\mathrm{Li}(1_1^+)+\Sigma^0$ (solid line) and $^6\mathrm{He}(0_1^+)+\Sigma^+$ (dotted line) channels in the bound $^7_\Sigma\mathrm{Li}$ state, and (b) respective Σ-nucleus imaginary potentials.
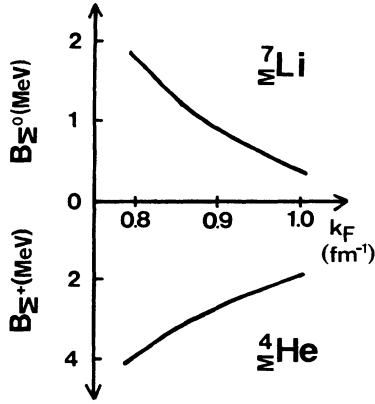
FIG. 6. Dependence of the nuclear Fermi momentum k_F for the YNG-D Σ-N interaction on the binding energies of $^7_\Sigma$Li and $^4_\Sigma$He.

fm^{-1}, the binding energy of $^7_\Sigma$Li ($^4_\Sigma$He) changes from 1.8 (4.0) to 0.4 (1.9) MeV and the conversion width of $^7_\Sigma$Li ($^4_\Sigma$He) changes from 6.4 (8.7) to 3.6 (5.9) MeV. It should be noted that the analysis of the light Λ hypernuclei with use of the YNG Λ-N interaction suggests a reasonable value of k_F from 0.8 to 1.0 fm^{-1} [17]. Therefore, even if we take into account both the uncertainty of the effective Σ-N interaction and the experimental error of the $^4_\Sigma$He binding energy, our result that there appears one bound state of $^7_\Sigma$Li with no large width does not change seriously.

In the present calculation, we did not find the bound $J^\pi = \frac{3}{2}^+$ state which consists of the $[^6\text{Li}(1^+_1) \otimes \Sigma^0]$ ($s = 1$, $t = 0$) and $[^6\text{He}(0^+_1) \otimes \Sigma^+]$ ($s = 0$, $t = 1$) configurations. The reason is given as follows: In the case of no channel coupling, the calculated eigenstate of $[^6\text{Li}(1^+_1) \otimes \Sigma^0]_{J^\pi = 3/2^+}$ appears at E_{Σ^0} ($= -B_{\Sigma^0}) \approx 1$ MeV. It should be reminded that the $[^6\text{Li}(1^+_1) \otimes \Sigma^0]_{J^\pi = 1/2^+}$ state appears at $E_{\Sigma^0} \approx 0$ MeV. The energy difference is due to the repulsive character of the spin-spin term of Σ-N interaction which works for the channel with the nuclear core spin $s = 1$. Concerning the $[^6\text{He}(0^+_1) \otimes \Sigma^+]$ channel, the calculated energy for the $J^\pi = \frac{3}{2}$ state is $E_{\Sigma^0} \approx 5$ MeV, while that for the $J^\pi = \frac{1}{2}$ state is $E_{\Sigma^0} \approx 1$ MeV. The large energy difference comes from the fact that the relative orbital angular momentum between $^6\text{He}(0^+_1)$ and Σ^+ is mainly $\lambda = 0$ and 2 in the $J^\pi = \frac{1}{2}^+$ and $\frac{3}{2}^+$ states, respectively. Owing to the same reason, the coupling matrix element between the $[^6\text{Li}(1^+_1) \otimes \Sigma^0]$ and $[^6\text{He}(0^+_1) \otimes \Sigma^+]$ channels in the $J^\pi = \frac{3}{2}^+$ state becomes smaller than that in the $J^\pi = \frac{1}{2}^+$ state. When the $[^6\text{Li}(1^+_1) \otimes \Sigma^0]_{J^\pi = 3/2^+}$ and $[^6\text{He}(0^+_1) \otimes \Sigma^+]_{J^\pi = 3/2^+}$ channels are coupled, the energy gain should not be larger than that in the case of $J^\pi = \frac{1}{2}^+$. As a result, there do not appear bound $J^\pi = \frac{3}{2}^+$ states with the $[^6\text{Li}(1^+_1) \otimes \Sigma^0]$ and $[^6\text{He}(0^+_1) \otimes \Sigma^+]$ configurations. On the other hand, we did not find the bound $J^\pi = \frac{5}{2}^+$ state with the $[^6\text{Li}(1^+) \otimes \Sigma^0(d_{5/2,3/2})]$ and $[^6\text{He}(0^+) \otimes \Sigma^+(d_{5/2})]$

configurations in the present calculation. This is due to the fact that the relative angular momentum between nuclear core and Σ particle is $\lambda = 2$.

IV. CONCLUSION

The possible existence of bound $^7_\Sigma$Li states was investigated within the frame of the microscopic $\alpha +$ "$2N$" $+ \Sigma$ cluster model by employing the effective Σ-N interaction which reproduces the experimental binding energy and width of $^4_\Sigma$He. We found the plausible $^7_\Sigma$Li bound state with $B_{\Sigma^0} = 1.2$ MeV and $\Gamma \approx 5.4$ MeV. The width comes only from the conversion process $\Sigma N \to \Lambda N$ because of the bound state. The bound state shows the mixed charge states with about 83% of total isospin $I = 1$, which consists of the $[^6\text{Li}(1^+_1) \otimes \Sigma^0]$ and $[^6\text{He}(0^+_1) \otimes \Sigma^+]$ configurations. This is in contrast with the fact that the $^4_\Sigma$He bound state is an almost pure isospin $I = \frac{1}{2}$ state.

The reason why such a bound state appears in $^7_\Sigma$Li is summarized as follows: Each eigenstate with no channel coupling appears around each threshold reflecting the characteristic of the weak attraction of each Σ-nucleus folding potential. The coupling potential between the $[^6\text{Li}(1^+_1) \otimes \Sigma^0]$ and $[^6\text{He}(0^+_1) \otimes \Sigma^+]$ states comes only from the $(\mathbf{t}_N \cdot \mathbf{t}_\Sigma)(\mathbf{s}_N \cdot \mathbf{s}_\Sigma)$ term of Σ-N interaction since the $(\mathbf{t}_N \cdot \mathbf{t}_\Sigma)(\mathbf{s}_N \cdot \mathbf{s}_\Sigma)$ term plays a role of coupling between the state with nuclear-core spin $s = 1$ and isospin $t = 0$ $[^6\text{Li}(1^+_1)]$ and the state with $s = 0$ and $t = 1$ $[^6\text{He}(0^+_1)]$. The coupling strength is much larger than the energy difference (about 1 MeV) between the $[^6\text{Li}(1^+_1) \otimes \Sigma^0]$ and $[^6\text{He}(0^+_1) \otimes \Sigma^+]$ states. Therefore, the two states are coupled strongly to produce the bound state. On the other hand, the Lane potential which couples only the state with the nuclear-core isospin $t = 1$ comes only from the $(\mathbf{t}_N \cdot \mathbf{t}_\Sigma)$ term of Σ-N interaction. The strength of the Lane potential is relatively smaller than the energy differences among the $[^6\text{He} \otimes \Sigma^+]$, $[^6\text{Li} \otimes \Sigma^0]$, and $[^6\text{Be} \otimes \Sigma^-]$ states with the nuclear-core isospin $t = 1$. Therefore, the three states are not coupled strongly. After all, the $^7_\Sigma$Li bound state, which is composed of the $[^6\text{Li}(1^+_1) \otimes \Sigma^0]$ and $[^6\text{He}(0^+_1) \otimes \Sigma^+]$ configurations, appears mainly due to the $(\mathbf{t}_N \cdot \mathbf{t}_\Sigma)(\mathbf{s}_N \cdot \mathbf{s}_\Sigma)$ term of the Σ-N interaction. It should be reminded that the $^4_\Sigma$He hypernucleus is bound mainly due to the cooperative role of the $(\mathbf{t}_N \cdot \mathbf{t}_\Sigma)$ and $(\mathbf{t}_N \cdot \mathbf{t}_\Sigma)(\mathbf{s}_N \cdot \mathbf{s}_\Sigma)$ term of the Σ-N interaction. The different binding mechanism between the $^7_\Sigma$Li and $^4_\Sigma$He hypernuclei comes from the different nuclear-core spin and isospin of the respective Σ hypernuclei $[(s,t) = (0,1),(1,0)$ for ^6He-^6Li-^6Be and $(s,t) = (\frac{1}{2}, \frac{1}{2})$ for ^3H-$^3\text{He}]$.

In conclusion, we have shown the possibility of a bound $^7_\Sigma$Li state which is produced mainly by the $(\mathbf{t}_N \cdot \mathbf{t}_\Sigma)(\mathbf{s}_N \cdot \mathbf{s}_\Sigma)$ term of Σ-N interaction. If the Σ hypernucleus is observed, we can get direct information on the $(\mathbf{t}_N \cdot \mathbf{t}_\Sigma)(\mathbf{s}_N \cdot \mathbf{s}_\Sigma)$ term of Σ-N interaction from the binding energy of $^7_\Sigma$Li. Therefore, it is highly desired that a hypernuclear production experiment such as a $^7\text{Li}(K^-, \pi^-)^7_\Sigma$Li reaction will be performed to study the possible existence of the bound $^7_\Sigma$Li hypernucleus.

[1] R. Bertini et al., Phys. Lett. 90B, 375 (1980); 136B, 29 (1984); 158B, 19 (1985).

[2] H. Piekarz et al., Phys. Lett. 110B, 428 (1982).

[3] C. B. Dover, D. J. Millener, and A. Gal, Phys. Rep. 184, 1 (1989).

[4] H. Bandō, T. Motoba, and J. Zofka, Int. J. Mod. Phys. A 5, 4021 (1990).

[5] E. Oset, P. Fernandez de Cordoba, L. L. Salcedo, and R. Brockmann, Phys. Rep. 188, 79 (1990).

[6] A. Gal and C. B. Dover, Phys. Rev. Lett. 44, 379 (1980).

[7] L. S. Kisslinger, Phys. Rev. Lett. 44, 968 (1980).

[8] J. Dabrowski and J. Rozynek, Phys. Rev. C 23, 1706 (1981).

[9] R. Brockmann and E. Oset, Phys. Lett. 118B, 33 (1982).

[10] J. A. Johnstone and A. W. Thomas, Nucl. Phys. A392, 409 (1983).

[11] K. Ikeda and T. Yamada, Int. J. Mod. Phys. A 3, 2339 (1988).

[12] R. S. Hayano, T. Ishikawa, M. Iwasaki, H. Outa, E. Takada, H. Tamura, A. Sakaguhi, M. Aoki, and T. Yamazaki, Phys. Lett. B 231, 355 (1989).

[13] T. Harada, S. Shinmura, Y. Akaishi, and H. Tanaka, Soryusiron Kenkyu (circular in Japanese) 76, 25 (1987); Nucl. Phys. A507, 715 (1990).

[14] T. Yamada and K. Ikeda, Nuovo Cimento 102A, 481 (1989).

[15] T. Yamada and K. Ikeda, Prog. Theor. Phys. 88, 139 (1992).

[16] M. M. Nagels, T. A. Rijken, and J. J. de Swart, Phys. Rev. D 12, 744 (1975); 15, 2547 (1977); 20, 1633 (1979).

[17] Y. Yamamoto and H. Bandō, Prog. Theor. Phys. Suppl. 81, 9 (1985); Y. Yamamoto, private communication.

[18] S. Saito, Prog. Theor. Phys. 40, 893 (1968); 41, 705 (1969); Prog. Theor. Phys. Suppl. 62, 11 (1977).

[19] H. Horiuchi, Prog. Theor. Phys. Suppl. 62, 90 (1977).

[20] T. Motoba, H. Bandō, K. Ikeda, and T. Yamada, Prog. Theor. Phys. Suppl. 81, 42 (1985).

[21] H. Nishioka, S. Saito, and M. Yasuno, Prog. Theor. Phys. 62, 424 (1979).

[22] F. Ajzenberg-Selove, Nucl. Phys. A320, 1 (1979).